Chemical Science

ROYAL SOCIETY OF CHEMISTRY

EDGE ARTICLE

View Article Online
View Journal | View Issue

Open Access Article. Published on 28 juli 2025. Downloaded on 29.9.2025 23:58:57.
This article is licensed under a Creative Commons Attribution-NonCommercial 3.0 Unported Licence.

Check for updates

Cite this: *Chem. Sci.*, 2025, **16**, 15964

All publication charges for this article have been paid for by the Royal Society of Chemistry

A cooperative electron-deficient phosphine/olefin ligand system for the site-selective mechanochemical Suzuki–Miyaura cross-coupling of 2,4-dibromoaryl ethers†

Yunpeng Gao,[a] Julong Jiang,[b] Satoshi Maeda,[bc] Koji Kubota *[ab] and Hajime Ito *[ab]

The palladium-catalyzed site-selective cross-coupling of identical halogen groups with minimal electronic and steric bias remains a formidable challenge, especially for simple benzene derivatives. Here, we report a cooperative phosphine/olefin ligand system that allows the unprecedented C2-selective Suzuki–Miyaura cross-coupling of 2,4-dibromoaryl ethers; regioselective reactions of these substrates are typically difficult to accomplish due to the small steric and electronic differences between the two bromo groups. The electron-deficient ligand JackiePhos facilitates the selective oxidative addition of the slightly-more-negatively-charged C2–Br bond, while 1,5-cyclooctadiene (1,5-cod) stabilizes the sensitive monomeric palladium species, preventing the *in situ* formation of ligand-less dense and large palladium aggregates that lead to nonselective cross-coupling. This unique ligand effect is more pronounced under solid-state ball-milling conditions than conventional solution-based conditions. Moreover, we demonstrate that by starting with the C2-selective cross-coupling, a sequential assembly of different aryl groups to the C2, C4, and even C1-site of the benzene core is possible, thus providing a straightforward and efficient strategy to construct multi-functionalized arene scaffolds.

Received 3rd March 2025
Accepted 24th July 2025

DOI: 10.1039/d5sc01669j

rsc.li/chemical-science

Introduction

The nobel-prize-winning palladium-catalyzed Suzuki–Miyaura cross-coupling has been demonstrated to be a tremendously powerful tool for the rapid construction of value-added molecules.[1] The demand for precise synthesis in pharmaceuticals, materials science, and other related research areas necessitates the development of predictable site-selective cross-coupling reactions for the efficient structure-diversification of polyhalogenated (hetero)arenes through stepwise functionalization (Scheme 1).[2] Polyhaloarene starting materials with identical halogens are preferable to those with non-identical ones,[3] predominantly due to their greater ease of accessibility (Scheme 1A). However, the site- and monoselective[4] cross-coupling of the identical halogen groups is challenging, and unwanted overarylation must be suppressed. One common method to achieve such site- and mono-selectivity is the use of substrates with a large electronic[5] or steric[6] bias, especially in the case of simple benzene derivatives (Scheme 1B). Another well-established substrate-controlled strategy is the incorporation of a directing group (DG) (Scheme 1C).[7] In this approach, the DGs coordinate to a palladium catalyst, which enables the selective functionalization of the proximal halogen group.[8] Related to this approach, Phipps and coworkers have investigated the site-selective coupling of polychlorinated benzenes directed by substrate–ligand electrostatic interactions.[9] However, despite these elegant advances, the DG strategy still suffers from laborious preinstallation procedures and limited generality.

In addition to the aforementioned substrate-controlled strategies, a catalyst-controlled approach[2c,10] would provide a general and complementary solution for the site-selective cross-coupling of identical halogen groups in various aromatic compounds. Previous studies have revealed that systematic catalyst modifications lead to unconventional site-selectivity in palladium-catalyzed cross-couplings of polyhalogenated heteroarenes.[11] However, the development of catalytic systems that enable site-selective Suzuki–Miyaura cross-coupling of unbiased polyhalogenated benzene derivatives remains unexplored. Inspired by recent significant advances in cross-coupling

[a]Division of Applied Chemistry and Frontier Chemistry Center, Faculty of Engineering, Hokkaido University, Sapporo, Hokkaido, Japan. E-mail: kbt@eng.hokudai.ac.jp; hajito@eng.hokudai.ac.jp

[b]Institute for Chemical Reaction Design and Discovery (WPI-ICReDD), Hokkaido University, Sapporo, Hokkaido, Japan

[c]Department of Chemistry, Faculty of Science, Hokkaido University, Sapporo, Hokkaido, Japan

† Electronic supplementary information (ESI) available. CCDC 2299550–2299553. For ESI and crystallographic data in CIF or other electronic format see DOI: https://doi.org/10.1039/d5sc01669j

© 2025 The Author(s). Published by the Royal Society of Chemistry

Open Access Article. Published on 28 juli 2025. Downloaded on 29.9.2025 23:58:57.
This article is licensed under a Creative Commons Attribution-NonCommercial 3.0 Unported Licence.

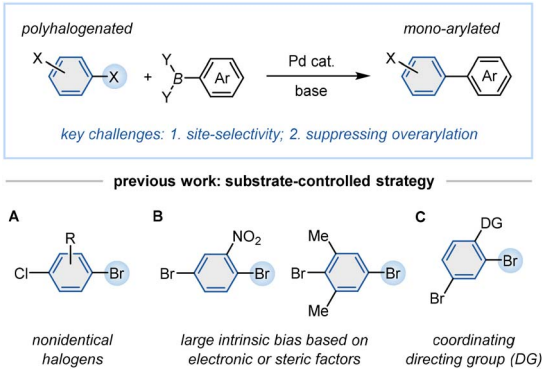

Scheme 1 Substrate-controlled site-selective Suzuki–Miyaura cross-coupling of polyhalogenated benzenes.

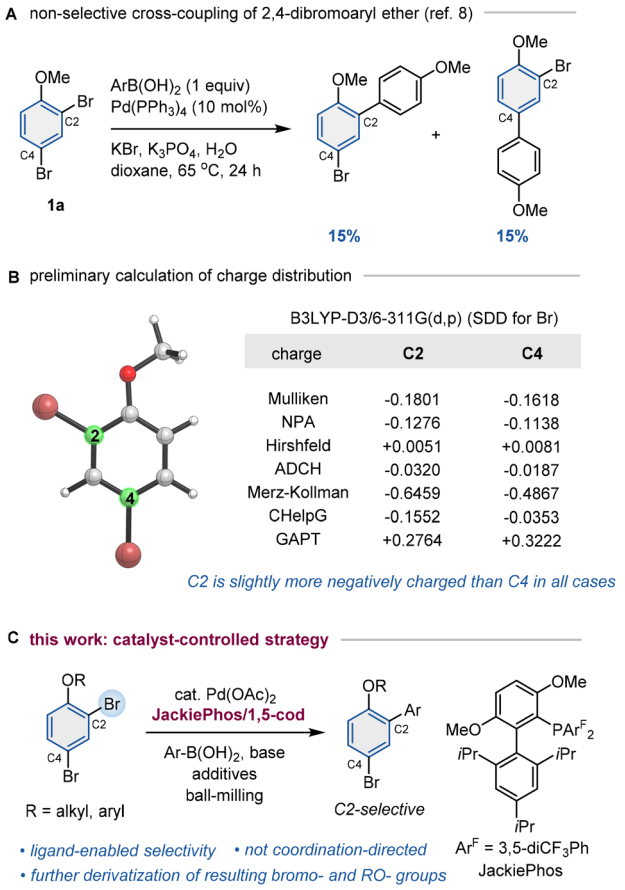

Scheme 2 Experimental and calculated reactivity of 2,4-dibromoaryl ethers.

chemistry, we envisioned that careful tuning of the electronic and steric properties of palladium catalysts could lead to conceptually new catalysts for the site- and mono-selective cross-coupling of polyhalogenated benzenes with small electronic and steric biases.

Ether is one of the most ubiquitous functional groups in natural products, drugs, and materials.[12] In particular, aryl ethers are useful synthetic intermediates, as they can be readily transformed into polyaromatics *via* nickel-catalyzed cross-coupling or into phenols or triflate derivatives,[13] which provides a starting point for various diversification routes. Therefore, the site-selective Suzuki–Miyaura cross-coupling of polyhalogenated aryl ethers would represent a powerful strategy for the construction of highly functionalized aryl ethers and structurally complex polyaromatics. However, control of the site-selectivity for this class of substrates represents a formidable challenge. The weak coordination ability of the ether group to the palladium catalyst makes coordination-assisted proximal cross-coupling difficult (*vide infra*).[14,15] Furthermore, the relatively weak electronic bias induced by an alkoxy group would not be sufficiently large to achieve site-selective coupling. In fact, Suzuki–Miyaura cross-coupling of the substrate 2,4-dibromoanisole (**1a**) under representative conditions using $Pd(PPh_3)_4$ as the catalyst resulted in a mixture of products with no site-selectivity (Scheme 2A).[8] This result suggests that the overall electronic and steric bias of the C2 and C4 sites is negligible. Therefore, as part of our research into the development of new site-selective palladium-based catalysts, we decided to focus on the Suzuki–Miyaura cross-coupling of 2,4-dibromoaryl ethers as a model reaction to investigate whether the site-selective cross-coupling of identical halogen groups with minimal inherent bias could be achieved *via* catalyst development.

We first sought to evaluate the electronic properties of 2,4-dibromoanisole (**1a**) using population analysis to quantify the electronic bias of the C2 and C4 positions (Scheme 2B).[16] Calculations using different methods universally showed the same trend, *i.e.*, that the C2 position is consistently more negatively charged than the C4 position. Generally, the most electrophilic carbon preferentially participates in the oxidative addition, which indicates that reaction at C4 should be favored over reaction at C2.[17] However, these results also suggest that the more negatively charged C2=C3 may have better coordination ability to the palladium catalyst than C4=C5 or C3=C4. Therefore, we envisioned that this small electronic bias between the C2 and C4 positions could be selectively recognized by the electron-deficient palladium catalyst, thus leading to unprecedented C2-selective cross-coupling.

In this work, we discovered that the electron-deficient phosphine/1,5-cod cooperative ligand system efficiently promotes Suzuki–Miyaura cross-coupling at the C2 position of 2,4-dibromoaryl ethers while minimizing unwanted overarylation (Scheme 2C). Experimental and theoretical investigations suggest a compelling cooperative effect between the two applied ligands, whereby the electron-deficient JackiePhos distinguishes two sites by selective π-coordination and 1,5-cod stabilizes the active catalytic species to prevent the formation of large palladium aggregates without ligands, which would lead to unwanted nonselective arylation. Interestingly, we observed a more pronounced cooperative ligand effect under solid-state ball-milling conditions than under conventional solution-based conditions, providing a solvent-less and sustainable protocol for site-selective cross-coupling technology. Mechanochemical synthesis offers a unique reaction environment with distinct kinetics and catalyst behavior.[18] The present study

Open Access Article. Published on 28 juli 2025. Downloaded on 29.9.2025 23:58:57.
This article is licensed under a Creative Commons Attribution-NonCommercial 3.0 Unported Licence.

highlights the potential of mechanochemistry as a powerful platform for advancing site-selective cross-coupling methodologies beyond what is achievable in solution-phase systems.

Results and discussion

Based on the population analysis of 2,4-dibromoanisole (**1a**), we began our investigation by evaluating the ligand effects in the Suzuki–Miyaura cross-coupling of **1a** and *p*-tolylboronic acid (**2a**) as a benchmark test reaction (Table 1). Combinations of $Pd(OAc)_2$ with different phosphine ligands were examined, and the resulting product ratios under solution-based conditions were compared. For the ligand-free reaction conducted in toluene under an inert atmosphere, the C4-arylated product (**4a**) was obtained as the major product with poor C2/C4-selectivity (Table 1, entry 1; C2/C4 = 33 : 67). The addition of various phosphine ligands (**L1–L7**) led to varied conversions, but the site-selectivity was unsatisfactory in most cases (Table 1, entries 2–8). We found that the use of the electron-deficient biaryl phosphine ligand JackiePhos (**L1**; Table 1, entry 2), which has been developed by Buchwald,[19] provides the highest C2-selectivity (C2/C4 = 81 : 19). Importantly, the use of electron-rich Buchwald ligands that bear the same biaryl scaffold, such as BrettPhos (**L2**; Table 1, entry 3) and *t*BuBrettPhos (**L3**; Table 1, entry 4), resulted in non-site-selective cross-coupling, and C4-arylated **4a** was obtained as the major product. These results suggest that the P-bound electron-withdrawing 3,5-(bis)trifluoromethylphenyl groups are crucial for achieving C2 selectivity. However, reactions using the strongly electron-deficient monodentate phosphine tris[3,5-bis(trifluoromethyl)phenyl]phosphine (**L4**; Table 1, entry 5) exhibited a lower conversion and no selectivity (C2/C4 = 50 : 50), suggesting that the electron-rich biaryl scaffold is necessary to ensure high conversion. Several of the phosphine ligands tested (**L5–L7**) had been previously reported to be highly active for

Table 1 Investigation of the reaction conditions[a]

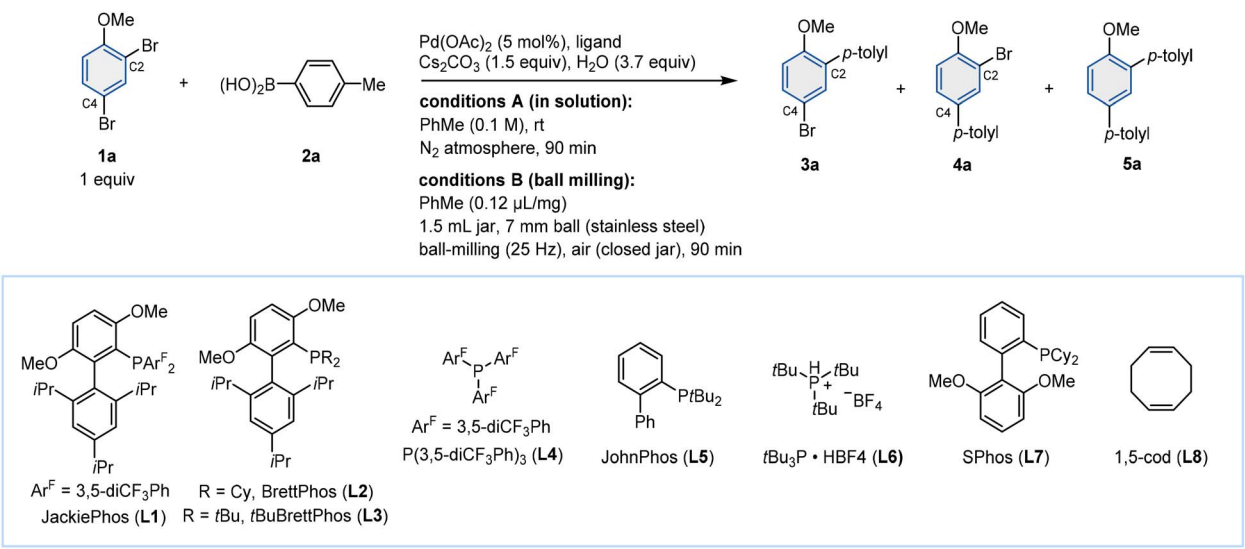

Entry	Ligand	Conditions (A/B)	**2a** (equiv)	Conv. of **1a** (%)	Yield of **3a** (%)	Yield of **4a** (%)	Yield of **5a** (%)	C2/C4 ratio
1	—	A	1.0	58	17	33	8	33 : 67
2	**L1** (5.5 mol%)	A	1.0	81	46	11	14	81 : 19
3	**L2** (5.5 mol%)	A	1.0	37	8	18	11	31 : 69
4	**L3** (5.5 mol%)	A	1.0	11	4	7	0	36 : 64
5	**L4** (5.5 mol%)	A	1.0	18	9	9	0	50 : 50
6	**L5** (5.5 mol%)	A	1.0	78	20	32	26	38 : 62
7	**L6** (11 mol%)	A	1.0	58	5	19	34	21 : 79
8	**L7** (5.5 mol%)	A	1.0	58	2	4	47	33 : 67
9	**L8** (15 mol%)	A	1.0	23	20	3	0	87 : 13
10	**L1** (5.5 mol%) + **L8** (15 mol%)	A	1.0	49	43	4	0	91 : 9
11	**L1** (5.5 mol%)	B	1.0	70	25	25	20	50 : 50
12	**L1** (5.5 mol%) + **L8** (15 mol%)	B	1.0	54	43	6	4	88 : 12
13[b,c]	**L1** (5.5 mol%) + **L8** (15 mol%)	A	1.8	57	47	6	4	89 : 11
14[b]	**L1** (5.5 mol%) + **L8** (15 mol%)	B	1.8	98	71	7	20	91 : 9

[a] Reactions were carried out at 0.15 mmol scale. Yields were determined by ^{1}H NMR spectroscopy using an internal standard. [b] Cs_2CO_3 (2.7 equiv). [c] Average result of three attempts.

 © 2025 The Author(s). Published by the Royal Society of Chemistry

Open Access Article. Published on 28 juli 2025. Downloaded on 29.9.2025 23:58:57.
This article is licensed under a Creative Commons Attribution-NonCommercial 3.0 Unported Licence.

Suzuki–Miyaura coupling. JohnPhos (**L5**; Table 1, entry 6) was characterized by high conversion of **1a** and **2a**, but the site- and mono-selectivity were both very poor. In the cases of tBu$_3$P (**L6**; Table 1, entry 7) and SPhos (**L7**; Table 1, entry 8), diarylated **5a** was obtained as the major product.

We have already reported that the use of 1,5-cyclooctadiene (1,5-cod; **L8**) as an additive significantly accelerates solid-state Suzuki–Miyaura cross-coupling reactions conducted under mechanochemical conditions.[20] Based on extensive mechanistic studies, we proposed that the coordination of this diene ligand[21] probably stabilizes the monomeric catalytically active species to suppress undesired catalyst aggregation, which might enhance the site-selectivity. In the present study, we found that the use of 15 mol% of **L8** (Table 1, entry 9) as the ligand resulted in high C2-selectivity (C2/C4 = 87 : 13) under solution conditions, although the yield of the products was poor (total 23%). We also found that the combination of **L1** and **L8** provides the highest C2-selectivity (Table 1, entry 10; C2/C4 = 91 : 9) and suppresses the generation of overarylated **5a**. Although combinations of other phosphine ligands and **L8** gave a somewhat improved selectivity, none outperformed the **L1**/**L8** system (for details, see the ESI†).

Table 2 Substrate scope of aryl boronic acids[a]

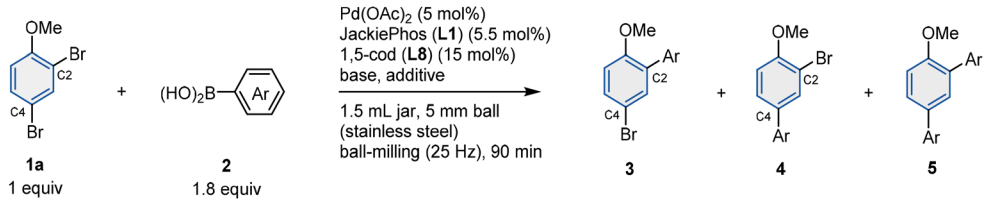

Entry	2	R	Desired product	NMR yield of 3 (%)	NMR yield of 4 (%)	NMR yield of 5 (%)	C2/C4 ratio	Isolated yield of 3 (%)
1	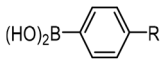	–Me (**2a**)	**3a**	71	7	20	91 : 9	62
2[b]		–H (**2b**)	**3b**	67	6	17	92 : 8	57
3		–Ph (**2c**)	**3c**	62	7	9	90 : 10	65
4		–tBu (**2d**)	**3d**	64	6	30	91 : 9	57
5		–OMe (**2e**)	**3e**	61	6	15	91 : 9	65 (92 : 8)
6		–NMe$_2$ (**2f**)	**3f**	59	7	6	89 : 11	55 (90 : 10)
7		–Cl (**2g**)	**3g**	58	6	8	91 : 9	53
8		–CF$_3$ (**2h**)	**3h**	64	6	18	91 : 9	53
9[c]		–CO$_2$Me (**2i**)	**3i**	64	6	16	91 : 9	58
10		–CN (**2j**)	**3j**	49	5	7	91 : 9	43
11	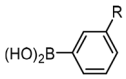	–Me (**2k**)	**3k**	68	6	28	92 : 8	57
12[c]		–Ac (**2l**)	**3l**	58	4	12	94 : 6	59
13[d]	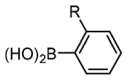	–Me (**2m**)	**3m**	72	6	17	92 : 8	69 (92 : 8)
14[d]		–iPr (**2n**)	**3n**	71	9	11	89 : 11	66 (89 : 11)
15		–OMe (**2o**)	**3o**	73	7	12	91 : 9	72 (91 : 9)
16[d]		–F (**2p**)	**3p**	70	6	22	92 : 8	55
17[d]	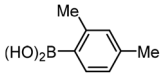	(**2q**)	**3q**	69	7	12	91 : 9	68 (90 : 10)
18	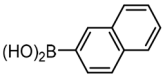	(**2r**)	**3r**	60	6	17	91 : 9	57
19[d]	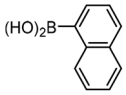	(**2s**)	**3s**	72	7	9	91 : 9	76 (91 : 9)
20[d]	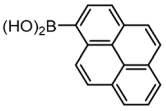	(**2t**)	**3t**	40	5	2	89 : 11	43 (90 : 10)

[a] Reactions were carried out at the 0.15 mmol scale. Unless otherwise noted, 1.8 equiv of **2** and 2.7 equiv of Cs_2CO_3 were used. Crude yields and C2/C4 ratios were determined by ^{1}H NMR spectroscopy using an internal standard. The isolated yield refers to pure **3** unless the regioisomeric ratio is noted in parentheses. For detailed reaction conditions, see the ESI. [b] **2** (1.4 equiv), Cs_2CO_3 (2.1 equiv). [c] **2** (1.6 equiv), Cs_2CO_3 (2.4 equiv). [d] **2** (2.4 equiv), Cs_2CO_3 (3.6 equiv), PhMe (0.24 μL mg^{-1}).

Open Access Article. Published on 28 juli 2025. Downloaded on 29.9.2025 23:58:57.
This article is licensed under a Creative Commons Attribution-NonCommercial 3.0 Unported Licence.

Solid-state cross-coupling reactions using ball-milling have been extensively explored in recent years due to their environmental friendliness and significantly higher efficiency compared to solution conditions.[22] Given that the effect of **L8** was originally discovered under mechanochemical conditions, we also investigated the cooperative ligand effect under solvent-free ball-milling conditions. Interestingly, while the $Pd(OAc)_2$/**L1** system showed C2-selectivity in solution (Table 1, entry 2), nonselective cross-coupling proceeded under mechanochemical conditions (Table 1, entry 11). However, we found that the cooperative ligand system with **L1** and **L8** provided high C2-selectivity (Table 1, entry 12, C2/C4 = 88 : 12). Furthermore, we subsequently carried out a preliminary catalyst screening to achieve the C4-selective Suzuki–Miyaura cross-coupling of **1a**. The highest yield of **4a** (44%) was afforded by the $Pd(OAc)_2$/QPhos/**L8** system, and the C2/C4 selectivity ratio was 21 : 79 (for details, see the ESI†). These preliminary results clearly demonstrate the ligand-controlled nature of the site-selectivity in the target cross-coupling reaction.

After determining the best ligand system, a brief optimization of the other parameters was carried out to improve conversion. Under solution conditions, increasing the loading of boronic acid **2a** (to 1.8 equiv) and the base Cs_2CO_3 (to 2.7 equiv) in toluene did not improve the conversion (Table 1, entry 13). The resulting yield of **3a** was low, and the reaction showed poor reproducibility (47%; average of three attempts). However, under ball-milling conditions, the highest yield of **3a** (71%) was achieved using the same loadings of **2a** and Cs_2CO_3, and the isomeric ratio was determined to be 91 : 9 (Table 1, entry 14). The improved results may be attributed to the better mixing of hydrophobic and hydrophilic reagents under ball-milling conditions, in contrast to the poor dispersion of the additive water under solution conditions (for details, see the ESI†). Thus, all subsequent investigations were conducted under solid-state ball-milling conditions.

To explore the substrate scope of this site-selective solid-state Suzuki–Miyaura cross-coupling, a variety of aryl boronic acids were tested (Table 2). The crude yields of C2-arylated product **3**, C4-arylated isomer **4**, and diarylated byproduct **5** were determined by ^{1}H NMR spectroscopy using the highly diagnostic methoxy peaks. In many cases, the target product **3** could be isolated by careful column chromatography on silica gel, while in other cases, inseparable mixtures of **3** and **4** were obtained (ratios are noted in parentheses). Although the use of 1.8 equiv of aryl boronic acid was suitable for most examples, fine tuning of this loading was often necessary to achieve a synthetically acceptable yield of **3**. For simple phenylboronic acid (**2b**), a loading of 1.4 equiv afforded **3b** in 67% yield, and the isomeric ratio was 92 : 8. Substituents at the C4 position of the aryl boronic acids (**2c–2i**) had little influence on the reaction outcome, giving good isolated yields of **3** (~60%) with good C2/C4 ratios (C2/C4 = 89 : 11–92 : 8), regardless of their electronic properties. Specifically, substrates with a phenyl group (**2c**) or bulky *tert*-butyl group (**2d**) at C4 led to moderate yields (62% and 64%) and good selectivity (C2/C4 = 90 : 10 and 91 : 9). Boronic acids with weakly coordinating methoxy (**2e**) and dimethylamino (**2f**) groups also participated in the coupling to give moderate yields (61% and 59%) and good site-selectivity (C2/C4 = 91 : 9 and 89 : 11). The chlorine group of **2g** remained intact after the coupling, and the corresponding product (**3g**; 58%, C2/C4 = 91 : 9) could participate in further functionalization. Electron-deficient trifluoromethyl (**2h**) and ester (**2i**) groups were both tolerated under the applied reaction conditions to afford the same yield (64%) and isomeric ratio (C2/C4 = 91 : 9). The reaction of 4-cyanophenyl boronic acid (**2j**) was slightly sluggish compared to other examples, and a 49% yield of **3j** (C2/C4 = 91 : 9) was obtained. Moving the methyl substituent from the C4 position to the C3 position had little effect on the efficiency, and the corresponding C2-arylated product (**3k**) was obtained in 68% yield with a high isomeric ratio (C2/C4 = 92 : 8). The carbonyl-functionalized substrate **2l** was tolerated by our system to give the desired product (**3l**) in moderate yield (58%) with the highest isomeric ratio (94 : 6) among all the tested examples. For C2-substituted aryl boronic acids (**2m–2q**, **2s–2t**), increasing the loading of **2** to 2.4 equiv led to the best results, perhaps due to their greater steric hindrance. The reaction of 2-methylphenyl boronic acid (**2m**) generated the C2-substituted product (**3m**) in 72% yield with an isomeric ratio of 92 : 8. Increasing the steric hindrance by replacing the methyl group with an isopropyl group (**2n**) resulted in slightly lower product selectivity (C2/C4 = 89 : 11), while the yield of **3n** was similar (71%). Good yields were also achieved for 2-methoxy (**2o**; 73%, C2/C4 = 91 : 9) and 2-fluoro (**2p**; 70%, C2/C4 = 92 : 8) phenyl boronic acids. 2,4-Dimethylphenyl boronic acid (**2q**) reacted successfully to afford the desired product (**3q**) in good yield (69%, C2/C4 = 91 : 9). Moreover, three fused polycyclic aryl boronic acids (**2r–2t**) were examined. The reaction of 2- and 1-naphthaleneboronic acids (**2r** and **2s**) with **1a** produced C2-arylated products **3r** and **3s** in 60% and 72% yield, respectively, with C2/C4 ratios of 91 : 9 in both cases. The yield of the coupling product **3t** (40%) from 1-pyreneboronic acid (**2t**) was significantly lower than for other examples, even though 2.4 equiv of **2t** was used. The isomeric ratio was also slightly diminished (C2/C4 = 89 : 11). The tested examples highlight the low relevance of the substituent pattern of the boronic acids for the site-selectivity. To further confirm the C2-arylated structure, single crystals of **3c** and **3r** were grown, and X-ray diffraction analysis verified our assignment (for details, see the ESI†).

Subsequently, we turned our attention to the scope of 2,4-dibromoaryl ether derivatives (Table 3). First, we investigated the effect of different alkoxy or aroxy groups. The substituent with an ethoxy group (**1b**) gave similar results to **1a**, generating **3u** in 63% yield and a C2/C4 ratio of 90 : 10. Glycol-derived 2,4-dibromo-1-(2-methoxyethoxy)benzene (**1b**) provided a slightly lower yield (60%) and isomeric ratio (C2/C4 = 87 : 13). Electron-deficient ether **1d**, which contains a trifluoroethoxy group, still preferentially underwent C2-arylation, delivering the corresponding product in 56% yield and 88 : 12 isomeric ratio. We also tested aroxy-bearing substrate **1e**. Because the lone electron pair of the oxygen atom is delocalized by the aromatic π-orbital, the aroxy group is a weaker electron donor than the alkoxy group. However, this electronic divergence has little influence on the reaction outcome, and the desired product (**3x**) was obtained in 58% yield with a good C2/C4 ratio (88 : 12). We found

 © 2025 The Author(s). Published by the Royal Society of Chemistry

Open Access Article. Published on 28 juli 2025. Downloaded on 29.9.2025 23:58:57.
This article is licensed under a Creative Commons Attribution-NonCommercial 3.0 Unported Licence.

Table 3 Substrate scope of 2,4-dibromoaryl ethers[a]

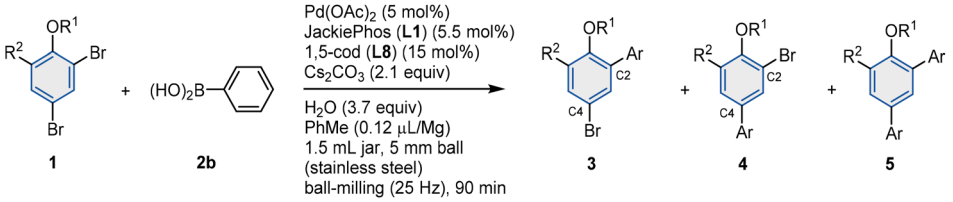

Entry	1	R^1 or R^2	Desired product	NMR yield of **3** (%)	NMR yield of **4** (%)	NMR yield of **5** (%)	C2/C4 ratio	Isolated yield of **3** (%)
1	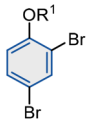	R^1 = –Et (**1b**)	**3u**	63	7	26	90 : 10	52
2		R^1 = –CH_2CH_2OMe (**1c**)	**3v**	60	9	21	87 : 13	59 (86 : 14)
3		R^1 = –CH_2CF_3 (**1d**)	**3w**	56	8	22	88 : 12	47
4		R^1 = –*p*-tolyl (**1e**)	**3x**	58	8	21	88 : 12	50
5		R^1 = –*t*Bu (**1f**)	**3y**	42	21	17	67 : 33	30
6	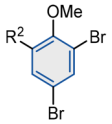	R^2 = –Me (**1g**)	**3z**	52	9	15	85 : 15	42
7[b]		R^2 = –CO_2Me (**1h**)	**3aa**	49	6	19	89 : 11	47
8	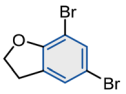	(**1i**)	**3ab**	67	6	–[c]	92 : 8	57

[a] Reactions were carried out at the 0.15 mmol scale. Unless otherwise noted, 1.4 equiv of **2** and 2.1 equiv of Cs_2CO_3 were used. Crude yields and C2/C4 ratios were determined by ^{1}H NMR spectroscopy using an internal standard. The isolated yield refers to pure **3** unless the regioisomeric ratio is noted in parentheses. For detailed reaction conditions, see the ESI. [b] **2** (1.8 equiv), Cs_2CO_3 (2.7 equiv). [c] Crude yield was not determined due to overlap of NMR peaks.

that the effect of steric hindrance was much larger than that of electronic factors. The introduction of a bulky *tert*-butoxy group (**1f**) lowered the site-selectivity (C2/C4 = 67 : 33), affording C2-arylated product **3y** in 42% yield. The steric bulk of the *tert*-butyl group possibly partially hampers the reaction at the proximate C2 position.

Next, an electron-donating methyl group (**1g**) and an electron-withdrawing ester group (**1h**) were introduced at the C6-position of the 2,4-dibromoanisole scaffold to investigate their impact on the reactivity. Both examples gave moderate product yields (**1g**; 52%; **1h**; 49%), and the C2/C4 ratio of **1g** (85 : 15) was slightly lower than that of **1h** (89 : 11). The reaction of a cyclic ether (**1i**) proceeded smoothly to give **3ab** in 57% isolated yield with a good isomeric ratio (92 : 8). The above results demonstrate that the ether substituents of the dibromoaryl ethers have a much greater effect on the site-selectivity than the structure of the boronic acids, suggesting that the oxidative-addition step of the ether substrate is decisive in terms of the site-selectivity, which is in good agreement with our working hypothesis.

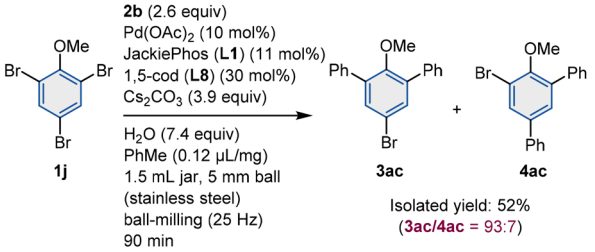

Scheme 3 Site-selective diarylation of 2,4,6-tribromoanisole **1j**.

Finally, we tested the reactivity of 2,4,6-tribromoanisole (**1j**) (Scheme 3). The introduction of an additional bromine atom significantly raises the complexity of the reaction outcomes, as five coupling products are possible. We found that the reaction could not be terminated after the first coupling in our initial attempts. A quick screening revealed that the use of 2.6 equiv of phenylboronic acid **2b** afforded diarylated product **3ac** in 52% isolated yield with excellent selectivity (**3ac**/**4ac** = 93 : 7).

In order to investigate the mechanistic origin of the unique C2-selectivity in our Pd/**L1**/**L8** system, we conducted DFT calculations of the oxidative-addition step at the B3LYP-D3/6-311G(d,p) level (Fig. 1). **L8** occupies the vacant coordination sites of the palladium center coordinated by **L1** to stabilize the active complex. After the dissociation of **L8**, the palladium complex is first coordinated by the substrate, followed by the oxidative addition of the C–Br bond to the Pd(0) center. The coordination of **1a** to the Pd center of Pd_Jakiephos affords **Pd_Ja_Int1A** (−20.4 kJ mol^{-1}) and **Pd_Ja_Int1B** (−3.0 kJ mol^{-1}). **Pd_Ja_Int1A** (−20.4 kJ mol^{-1}) is the more stable intermediate, supporting its role as the resting state prior to the oxidative addition. Once **Pd_Ja_Int1B** (−3.0 kJ mol^{-1}) is produced, this

Open Access Article. Published on 28 juli 2025. Downloaded on 29.9.2025 23:58:57.
This article is licensed under a Creative Commons Attribution-NonCommercial 3.0 Unported Licence.

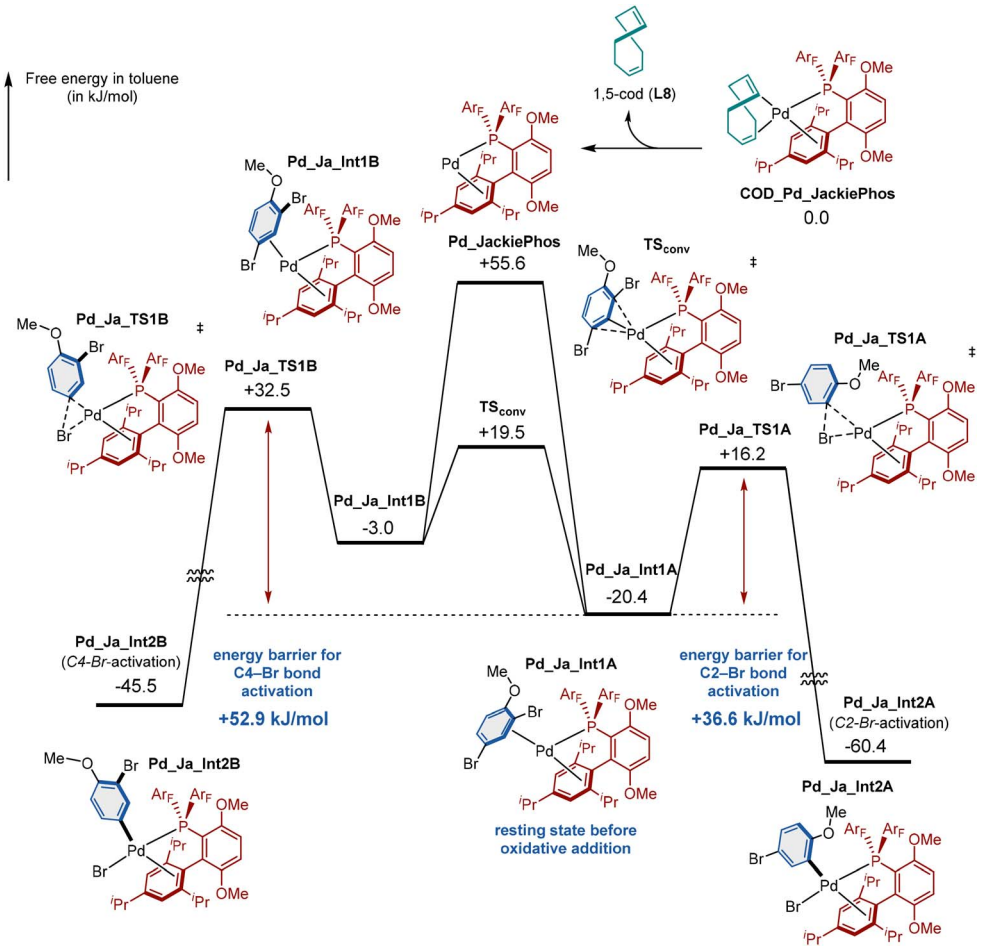

Fig. 1 DFT calculations for the oxidative-addition step of **1a** to Pd_JackiePhos. Relative Gibbs energy values (in kJ mol^{-1}) were calculated at the B3LYP-D3/6-311G(d,p)//B3LYP-D3/6-311G(d,p) level (SDD basis sets used for Br and Pd) using the implicit IEF-PCM solvation model (solvent = toluene).

intermediate can be converted to the thermodynamically more stable **Pd_Ja_Int1A** (−20.4 kJ mol^{-1}) through Pd migration on the benzene ring with a low activation barrier (22.5 kJ mol^{-1}). This interconversion is faster than the oxidative addition of the C4–Br bond from **Pd_Ja_Int1B** with an activation barrier of 35.5 kJ mol^{-1}. Collectively, these results confirm that oxidative addition at the C2 position is both kinetically and thermodynamically preferred, with a lower overall energy barrier (36.6 kJ mol^{-1}) compared to that at C4 (52.9 kJ mol^{-1}). Notably, direct coordination of the methoxy group to the palladium center does not take place at any point during the process. **L1** is an electron-deficient ligand, and thus, as we expected, coordination with the more negatively charged C2=C3 is greatly favored compared to coordination with C4=C5. Additional calculations based on the distortion–interaction model also show that, compared to **Pd_Ja_TS1B**, the interaction between the distorted Pd complex and 2,4-dibromoanisole is significantly stronger in **Pd_Ja_TS1A**. This result suggests that the observed C2-selectivity may be attributed to electronic effects (for details, see the ESI†).

To confirm the proposed site-selective oxidative-addition process, we carried out a stoichiometric reaction to synthesize the corresponding oxidative adduct (**6**) (Scheme 4A). A precatalyst that readily releases (**L8**)Pd(0) species *in situ*, (**L8**)Pd(CH_2TMS)$_2$, was used as the palladium source. The reaction of the palladium source, **1a**, and **L1** was first performed in solution. We found that the formed complex was stable enough to be isolated by flash chromatography on silica gel, providing 40% overall yield as a mixture of C2-oxidative-addition complex **6** and C4-oxidative-addition complex **7**. The C2/C4 isomeric ratio was determined to be 91 : 9 by ^{1}H NMR spectroscopy, which is in accordance with the catalytic reactions. Recrystallization of the mixture from pentane/dichloromethane afforded an orange single crystal that was analyzed by X-ray diffraction. The structure of the major isomer was unambiguously determined to be the C2-oxidative-addition complex **6**. High-resolution ESI-MS analysis confirmed our assignment of the structure (for details, see the ESI†). Next, a stoichiometric mechanochemical reaction was attempted (Scheme 4A). After 30 minutes of ball-milling in air, the corresponding products (**6** and **7**) were obtained in 34% isolated yield with the same

 © 2025 The Author(s). Published by the Royal Society of Chemistry

Open Access Article. Published on 28 juli 2025. Downloaded on 29.9.2025 23:58:57.
This article is licensed under a Creative Commons Attribution-NonCommercial 3.0 Unported Licence.

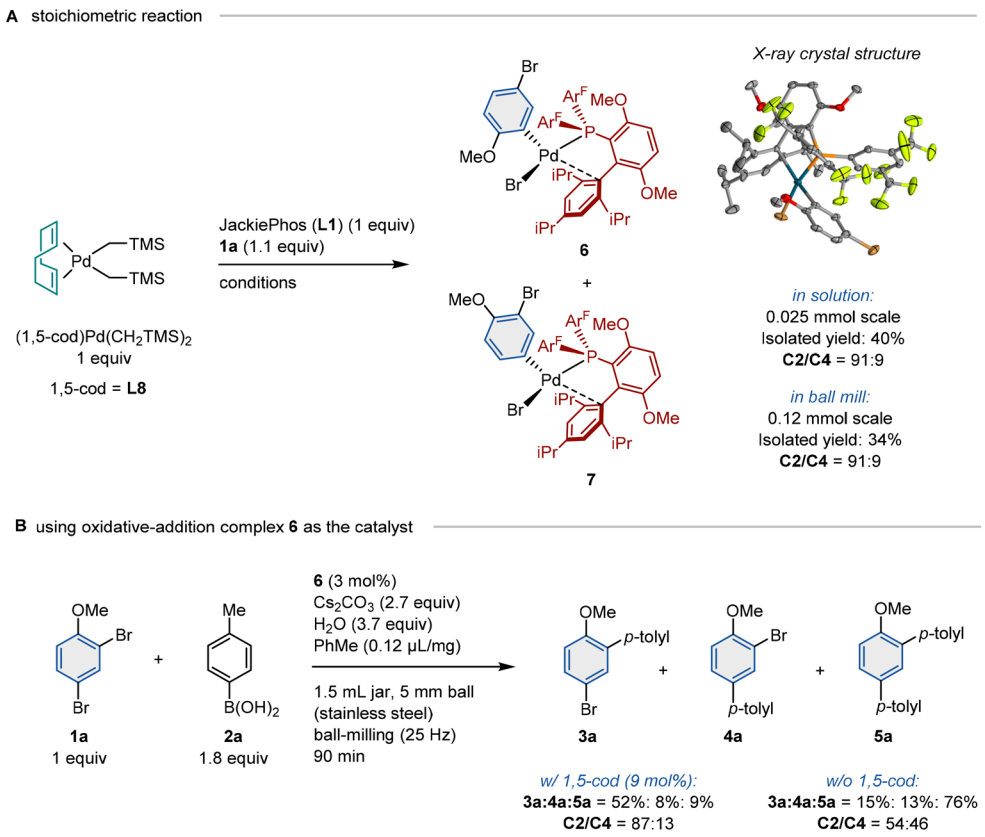

Scheme 4 Synthesis and reactivity of the oxidative–addition complex **6**.

Table 4 Comparison of the reactivity of the mono-arylated products toward overarylation[a]

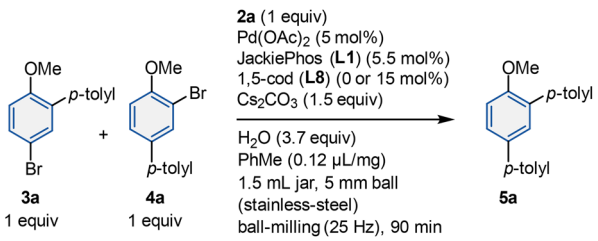

Entry	Amount of **L8**	Conv. of **3a** (%)	Conv. of **4a** (%)	Yield of **5a** (%)	Conv. ratio (**3a**/**4a**)
1	None	40	16	56	71 : 29
2	15 mol%	12	24	36	33 : 67

[a] Reactions were carried out at the 0.075 mmol scale. Crude yields were determined by ^{1}H NMR spectroscopy using an internal standard.

isomeric ratio (**6**/**7** = 91 : 9). These results are consistent with our calculations, which suggested that the site-selectivity is determined during the oxidative addition step, and that **L1** plays a key role in this process. Subsequently, we tested the catalytic reactivity of oxidative-addition complex **6** (Scheme 4B). The reaction between **1a** and **2a** in the presence of **6** as the catalyst with **L8** as an additional ligand afforded the desired product (**3a**) with good C2-selectivity (C2/C4 = 87 : 13), although the yield and isomeric ratio were lower than those under the optimized conditions. When **L8** was not added, diarylated product **5a** was obtained as the major product, and the reaction became nonselective. These observations are similar to the results under the standard catalytic conditions, indicating the involvement of oxidative addition complexes **6** and **7** in the actual catalytic cycle. Additionally, the influence of **L8** on the reaction outcome highlighted again.

In our calculated process, the weakly coordinated **L8** dissociates from the palladium center before the selectivity-

Open Access Article. Published on 28 juli 2025. Downloaded on 29.9.2025 23:58:57.
This article is licensed under a Creative Commons Attribution-NonCommercial 3.0 Unported Licence.

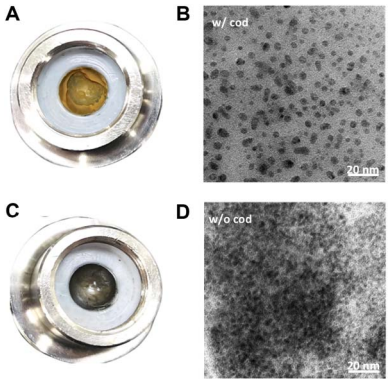

Fig. 2 Reaction mixtures and TEM images of the reaction mixture after 90 min of ball-milling: (A) and (B) mixture with **L8**; (C) and (D) mixture without **L8**; scale bar in the TEM images (bottom right): 20 nm.

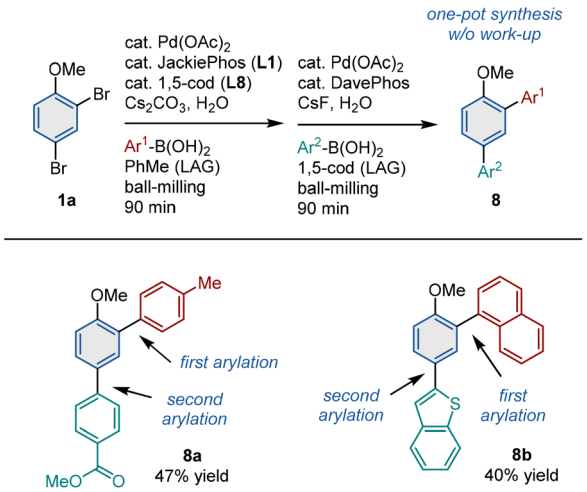

Scheme 5 One-pot sequential site-selective arylation under ball-milling conditions. [a]Reactions were carried out at the 0.15 mmol scale. Yields shown refer to isolated yields; for the detailed reaction conditions, see the ESI.†

determining oxidative-addition step, and thus, it cannot explain the significant influence of **L8** on the yield and site-selectivity. We inferred that **L8** might have profound effects on other uncalculated side processes. In order to obtain further mechanistic insight, the overarylation process was first investigated. Equimolar quantities of C2-arylated **3a**, C4-arylated **4a**, and boronic acid **2a** were subjected to the standard reaction conditions in order to quantify their relative reactivity toward overreaction (Table 4). When **L8** was absent (Table 4, entry 1), diarylated **5a** was generated in 56% yield, of which 40% stemmed from **3a**, and 16% from **4a**. When **L8** was added as a second ligand (Table 4, entry 2), the total conversion decreased to 36%, and the relative reactivity of the mono-arylated products was inverted. The consumption of undesirable **4a** was twice as large as that of the target product (**3a**). Hence, **L8** could slow the undesired overarylation of the target C2-coupled product.

Recently, Fairlamb and coworkers have reported that a mononuclear palladium complex and multinuclear palladium clusters/nanoparticles lead to different site-selectivity in coupling reactions of 2,4-dibromopyridine.[23] In this context, we inferred that **L8** may play a key role in stabilizing the C2-selective monomeric [JackiePhos(**L1**)]Pd(0) complex, thus suppressing aggregation of the catalyst to form large poorly selective or nonselective palladium aggregates without ligands. In fact, we noticed that an orange mixture was obtained after the benchmark reaction of **1a** and **2a** in the presence of L8, while the formation of palladium black was visually confirmed when L8 was not added to the mixture (Fig. 2A and C). To characterize the *in situ*-generated palladium aggregates, the crude mixtures were evenly dispersed in ethanol and then subjected to transmission electron microscopy (TEM) analysis. The mixture containing **L8** exhibited evenly dispersed multinuclear palladium nanoparticles (approximate size: 3–5 nm; Fig. 2B), which can be expected to have been formed during the sample preparation for TEM, while dense and large aggregates were generated in the absence of **L8** (Fig. 2D). These results indicate that **L8** can

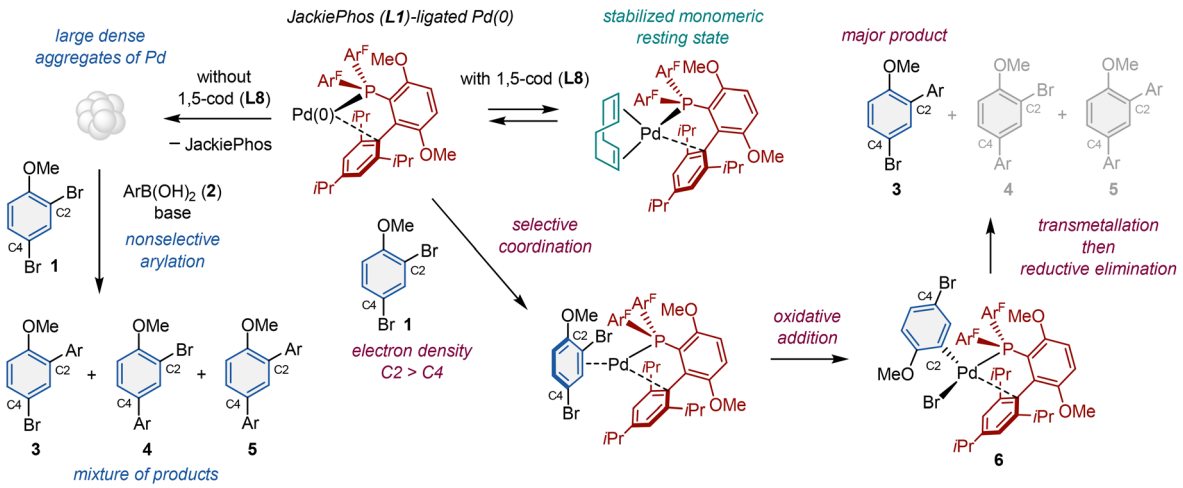

Fig. 3 Mechanistic rationale of the cooperative ligand effect for the selective cross-coupling of 2,4-dibromoaryl ethers.

 © 2025 The Author(s). Published by the Royal Society of Chemistry

Open Access Article. Published on 28 júlí 2025. Downloaded on 29.9.2025 23:58:57.
This article is licensed under a Creative Commons Attribution-NonCommercial 3.0 Unported Licence.

suppress the formation of dense and large palladium aggregates without ligands, which would not exhibit C2-selectivity in the cross-coupling.

Based on the mechanistic studies reported above, we summarized the role of the **L1**/**L8** dual-ligand system in the developed site-selective Suzuki–Miyaura cross-coupling as shown in Fig. 3. Considering the results of the DFT calculations, ligand screening, and stoichiometric reactions, we propose that electron-deficient **L1**-ligated palladium(0) enables the selective recognition of the more negatively charged C2 position of 2,4-dibromoaryl ether substrates, facilitating the C2-selective oxidative addition to form the C2-arylated products. From the control experiments and TEM analysis, we also propose that **L8**, which is a weakly-coordinating bidentate ligand, can occupy the remaining vacant sites of the **L1**-ligated palladium(0) complex to stabilize this monomeric active species, which greatly

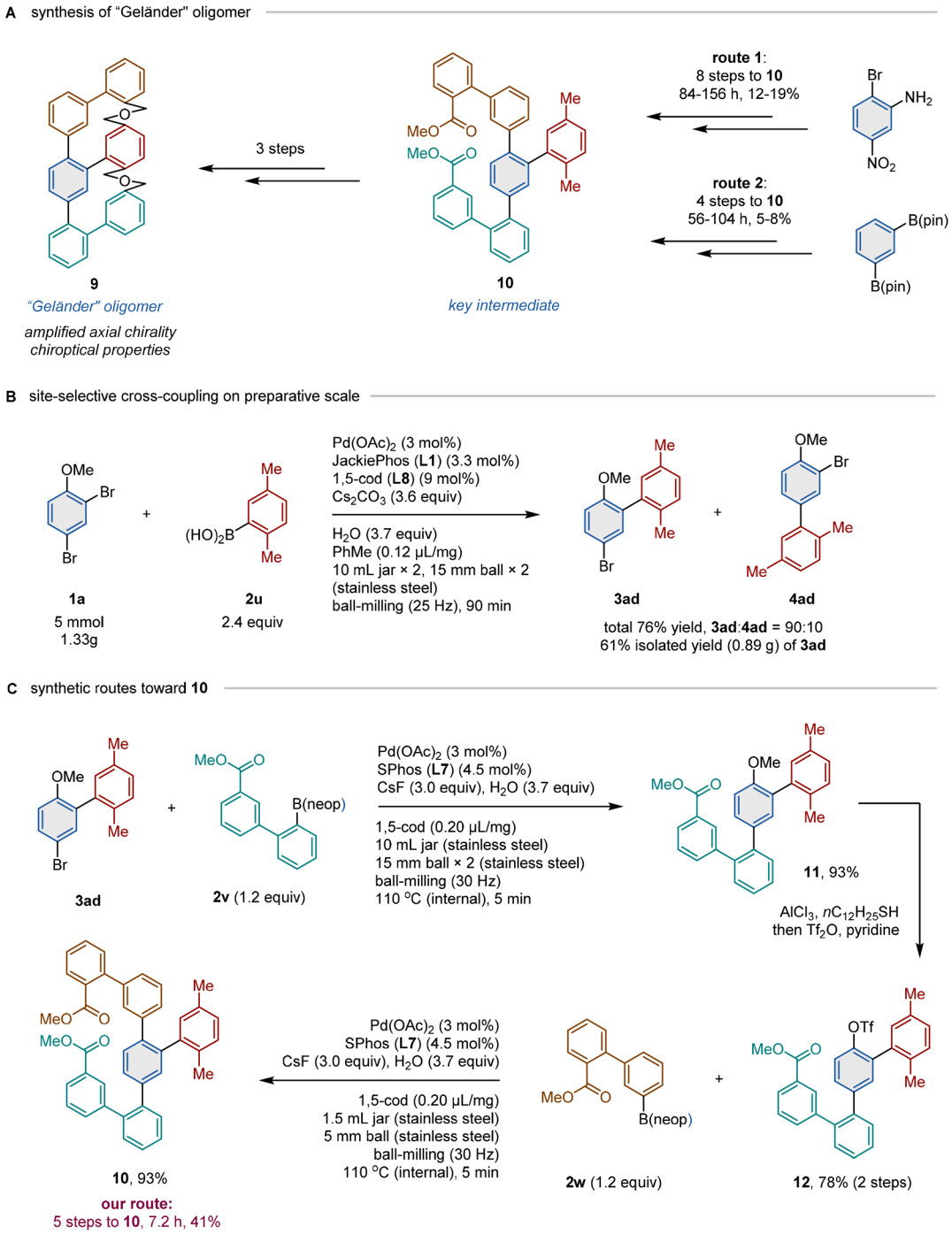

Scheme 6 "Geländer"-type oligomer **9** and synthetic routes toward key intermediate **10**.[a] (A) Synthesis of "Geländer"-type oligomer **9**. (B) Preparative-scale site-selective cross-coupling. (C) Synthesis of **10**. [a]Tf: triflate; neop: neopentyl glycolato; for detailed reaction conditions, see the ESI.†

Open Access Article. Published on 28 juli 2025. Downloaded on 29.9.2025 23:58:57.
This article is licensed under a Creative Commons Attribution-NonCommercial 3.0 Unported Licence.

suppresses the undesired aggregation of the catalyst to form poorly selective or nonselective multinuclear palladium nanoparticles. This ligand corporation was observed both in solution and under solid-state conditions using mechanochemistry, albeit the latter was found to be superior in terms of reproducibility.

To explore potential synthetic applications of this protocol, we developed a one-pot sequential site-selective arylation method to construct unsymmetrical terphenyl scaffolds (Scheme 5). After the first C2-selective arylation of **1a**, the milling jar was directly opened in air without work-up. A new ligand (DavePhos), CsF, additional **L8**, and another aryl boronic acid were added to the jar, and the contents were subjected to a second solid-state coupling. The $Pd(OAc)_2$/DavePhos/**L8** system is a general and effective combination to furnish the second arylation at the C4 position.[20] As shown in Scheme 5, two terphenyl products were isolated in moderate yield *via* this procedure (**8a**: 47%; **8b**: 40%). A single crystal of **8a** was analyzed using X-ray diffraction, and the results were consistent with the proposed structure (for details, see the ESI†).

After the successful one-pot construction of terphenyl compounds, we shifted our focus to the more challenging 1,2,4-trisubstituted targets. Mayor and coworkers have designed a novel "Geländer"-type oligomer (**9**) with a terphenyl backbone and an oligomer banister with oxy-gen-bridged benzyl subunits (Scheme 6A).[24] This stair-case-like structure can amplify the axial chirality of the backbone, leading to good chiroptical properties. The same group prepared an important intermediate (**10**) with three different aryl substituents located at the C1, C2, and C4 positions of the central phenyl core (Scheme 6A). The first synthetic route toward **10** includes the laborious incorporation of various leaving groups to the phenyl core as handles to distinguish different sites.[24,25] A subse-quent modification shortened the route. However, the troublesome selectivity issue significantly limited the overall yield of **9**.[26]

We envisioned that 2,4-dibromoanisole **1a** could serve as a low-cost, ready-to-use starting core for the construction of this complex scaffold. The first arylation was conducted on the gram scale employing our mechanochemical C2-selective cross-coupling method (Scheme 6B). This large-scale approach proceeded smoothly with a decreased catalyst loading (3 mol%) to generate 1.10 g of a mixture of the mono-arylated products (**3ad** + **4ad**) with a C2/C4 ratio of 90 : 10. Further purification afforded pure **3ad** in 61% isolated yield. The subsequent arylation of the resulting bromo group in **3ad** was accomplished within 5 min using a recently reported high-temperature ball-milling method (preset temperature: 250 °C, internal temperature: 110 °C) to give difunctionalized **11** in 93% isolated yield (Scheme 6C).[27] Unfortunately, our attempts at the nickel-catalyzed Suzuki–Miyaura cross-coupling of the methyl ether moiety of **11** failed.[28] Therefore, we pursued an alternative pathway involving the transformation of the methoxy group into a pseudohalogen, *i.e.*, a triflate group. *Ipso*-triflated intermediate **12** was obtained after the highly efficient chemoselective demethylation and triflation of **11** and then subjected to another high-temperature solid-state Suzuki–Miyaura cross-coupling. The same $Pd(OAc)_2$/SPhos (**L7**)/**L8** system was applied, and the target molecule (**10**) was obtained in 93% isolated yield. Notably, this is the first example to employ triflate in a high-temperature-accelerated solid-state cross-coupling, indicating the extraordinary generality and efficiency of this protocol. Compared to previous synthetic routes, our route is extraordinarily time-saving and efficient; specifically, owing to the fast and productive mechanochemical cross-couplings, the total reaction is at least eight times faster than hitherto reported routes, and the overall yield is 41%, which is 2–5 times higher than those of hitherto reported routes. The developed C2-selective coupling enables the functionalization of the C2, C4, and C1 sites of the 2,4-dibromoanisole core in a well-defined order, thus providing a general, straightforward, and streamlined protocol to construct unsymmetrical polyphenyl scaffolds.

Conclusions

In conclusion, we have developed a site-selective Suzuki–Miyaura cross-coupling for 2,4-dibromoaryl ethers, which is enabled by a cooperative ligand system. The combination of the ligands JackiePhos (**L1**) and 1,5-cod (**L8**) facilitates the C2-selective arylation for a wide variety of substituted aryl boronic acids and aryl ethers. Extensive mechanistic investigations revealed that the electron-deficient **L1**-ligated monomeric Pd(0) active species distinguishes between the C2 and C4 positions, despite their minimal electronic divergence, while **L8** acts as a stabilizer to prevent the aggregation of the palladium catalyst into dense multinuclear palladium aggregates without ligands, which would promote unwanted nonselective cross-coupling. The synthetic utility of this site-selective protocol was demonstrated by its applicability for the highly efficient synthesis of a "Geländer"-type oligomer, which provides a straightforward pathway to construct value-added trisubstituted arenes. We anticipate that the present study will inspire the development of site-selective cross-couplings of various substrates with minimal electronic and steric bias *via* rational catalyst design, particularly focusing on cooperative-ligand systems pairing an electron-deficient ligand with a stabilizing ligand. Further studies in this direction are currently in progress in our laboratory.[29]

Data availability

The data supporting this article have been included as part of the ESI.†

Author contributions

KK and HI conceived and designed the study. YG performed the chemical experiments and analysed the data. JJ and SM performed computational studies. All authors discussed the results and co-wrote the manuscript.

Conflicts of interest

There are no conflicts to declare.

 © 2025 The Author(s). Published by the Royal Society of Chemistry

Open Access Article. Published on 28 juli 2025. Downloaded on 29.9.2025 23:58:57.
This article is licensed under a Creative Commons Attribution-NonCommercial 3.0 Unported Licence.

Acknowledgements

This work was financially supported by the Japan Society for the Promotion of Science (JSPS) *via* KAKENHI grants 22H00318, 22K18333, 24H00453, 24H01832 and 24H01050, by the JST *via* CREST grant JPMJCR19R1, by FOREST grant JPMJFR201I, and by the Institute for Chemical Reaction Design and Discovery (ICReDD) established by the World Premier International Research Initiative (WPI), MEXT, Japan. We thank Mr. Yamato Fukuzawa for his help in cross-checking experiments.

Notes and references

1 (*a*) C. C. C. Johansson Seechurn, M. O. Kitching, T. J. Colacot and V. Snieckus, *Angew. Chem., Int. Ed.*, 2012, **51**, 5062–5085; (*b*) Á. Molnár, in *Palladium-Catalyzed Coupling Reactions: Practical Aspects and Future Development*, Wiley-VCH, Weinheim, Germany, 2013, pp. 1–30; (*c*) A. de Meijere and F. Diederich, in *Metal-Catalyzed Cross-Coupling Reactions*, 2nd edn, Wiley-VCH, Weinheim, Germany, 2008, pp. 41–123; (*d*) N. Miyaura and A. Suzuki, *Chem. Rev.*, 1995, **95**, 2457–2483; (*e*) A. J. J. Lennox and G. C. Lloyd-Jones, *Chem. Soc. Rev.*, 2014, **43**, 412–443; (*f*) R. Martin and S. L. Buchwald, *Acc. Chem. Res.*, 2008, **41**, 1461–1473.

2 (*a*) V. Palani, M. A. Perea and R. Sarpong, *Chem. Rev.*, 2022, **122**, 10126–10169; (*b*) J. Almond-Thynne, D. C. Blakemore, D. C. Pryde and A. C. Spivey, *Chem. Sci.*, 2017, **8**, 40–62; (*c*) K. Manabe and M. Yamaguchi, *Catalysts*, 2014, **4**, 307–320; (*d*) J.-R. Wang and K. Manabe, *Synthesis*, 2009, 1405–1427; (*e*) I. J. S. Fairlamb, *Chem. Soc. Rev.*, 2007, **36**, 1036–1045; (*f*) S. Schröter, C. Stock and T. Bach, *Tetrahedron*, 2005, **61**, 2245–2267; (*g*) R. Rossi, F. Bellina and M. Lessi, *Adv. Syn. Catal.*, 2012, **354**, 1181–1255; (*h*) A. R. Kapdi and D. Prajapati, *RSC Adv.*, 2014, **4**, 41245–41259.

3 (*a*) P. Dobrounig, M. Trobe and R. Breinbauer, *Monatsh. Chem.*, 2017, **148**, 3–35; (*b*) E. K. Reeves, E. D. Entz and S. R. Neufeldt, *Chem.–Eur. J.*, 2021, **27**, 6161–6177; (*c*) S. S. Ng, W. H. Pang, O. Y. Yuen and C. M. So, *Org. Chem. Front.*, 2023, **10**, 4408–4436.

4 (*a*) T. Seo, K. Kubota and H. Ito, *J. Am. Chem. Soc.*, 2020, **142**, 9884–9889; (*b*) D. J. Sinclair and M. S. Sherburn, *J. Org. Chem.*, 2005, **70**, 3730–3733; (*c*) C.-G. Dong, T.-P. Liu and Q.-S. Hu, *Synlett*, 2009, 1081–1086; (*d*) E. Guillén, J. Hierrezuelo, R. Martínez-Mallorquín, J. M. López-Romero and R. Rico, *Tetrahedron*, 2011, **67**, 2555–2561; (*e*) C. Minard, C. Palacio, K. Cariou and R. H. Dodd, *Eur. J. Org. Chem.*, 2014, **2014**, 2942–2955.

5 S. A. Kazi, E. M. Campi and M. T. W. Hearn, *Tetrahedron*, 2018, **74**, 1731–1741.

6 (*a*) C.-C. Lee, N. R. A. Amin, J.-J. Xu, B.-C. Wang, D. Luo, K. Sutanto, S. Biring, S.-W. Liu and C.-H. Chen, *J. Mater. Chem. C*, 2021, **9**, 9453–9464; (*b*) J. L. Gustafson, D. Lim, K. T. Barrett and S. J. Miller, *Angew. Chem., Int. Ed.*, 2011, **50**, 5125–5129.

7 (*a*) I. N. Houpis, C. Huang, U. Nettekoven, J. G. Chen, R. Liu and M. Canters, *Org. Lett.*, 2008, **10**, 5601–5604; (*b*) M. R. Cargill, G. Sandford, A. J. Tadeusiak, D. S. Yufit, J. A. K. Howard, P. Kilickiran and G. Nelles, *J. Org. Chem.*, 2010, **75**, 5860–5866; (*c*) D. Yu, Q. Shen and L. Lu, *J. Org. Chem.*, 2012, **77**, 1798–1804; (*d*) H. Hikawa and Y. Yokoyama, *Tetrahedron*, 2010, **66**, 9552–9559; (*e*) W. Yang, Y. Wang and J. R. Corte, *Org. Lett.*, 2003, **5**, 3131–3134.

8 For a unique distal C–X activation enabled by a directing-group strategy, see: P. Zhao, M. D. Young and C. M. Beaudry, *Org. Biomol. Chem.*, 2015, **13**, 6162–6165.

9 (*a*) W. A. Golding, R. Pearce-Higgins and R. J. Phipps, *J. Am. Chem. Soc.*, 2018, **140**, 13570–13574; (*b*) W. A. Golding, H. L. Schmitt and R. J. Phipps, *J. Am. Chem. Soc.*, 2020, **142**, 21891–21898; (*c*) I. K. W. On, W. Hong and Y. Zhu, *Tetrahedron Lett.*, 2023, **119**, 154408.

10 (*a*) J. Mahatthananchai, A. M. Dumas and J. W. Bode, *Angew. Chem., Int. Ed.*, 2012, **51**, 10954–10990; (*b*) C. Nájera, I. P. Beletskaya and M. Yus, *Chem. Soc. Rev.*, 2019, **48**, 4515–4618.

11 J. P. Norman and S. R. Neufeldt, *ACS Catal.*, 2022, **12**, 12014–12026.

12 T. Henkel, R. M. Brunne, H. Müller and F. Reichel, *Angew. Chem., Int. Ed.*, 1999, **38**, 643–647.

13 (*a*) M. Tobisu and N. Chatani, *Acc. Chem. Res.*, 2015, **48**, 1717–1726; (*b*) M. Tobisu and N. Chatani, *Top. Curr. Chem.*, 2016, **374**, 41; (*c*) Z. Qiu and C.-J. Li, *Chem. Rev.*, 2020, **120**, 10454–10515; (*d*) H. Diao, Z. Shi and F. Liu, *Synlett*, 2021, **32**, 1494–1512.

14 For a computational study, see:A. Tomberg, M. É. Muratore, M. J. Johansson, I. Terstiege, C. Sköld and P.-O. Norrby, *iScience*, 2019, **20**, 373–391.

15 For ether-directed palladium-catalyzed cross-couplings, only C–H activation is reported; for details, see:(*a*) G. Li, D. Leow, L. Wan and J.-Q. Yu, *Angew. Chem., Int. Ed.*, 2013, **52**, 1245–1247; (*b*) Á. Iglesias, R. Álvarez, Á. R. de Lera and K. Muñiz, *Angew. Chem., Int. Ed.*, 2012, **51**, 2225–2228.

16 (*a*) R. S. Mulliken, *J. Chem. Phys.*, 1955, **23**, 2343–2346; (*b*) A. E. Reed, R. B. Weinstock and F. Weinhold, *J. Chem. Phys.*, 1985, **83**, 735–746; (*c*) F. L. Hirshfeld, *Theor. Chim. Acta*, 1977, **44**, 129–138; (*d*) T. Lu and F. Chen, *J. Theor. Comput. Chem.*, 2012, **11**, 163–183; (*e*) U. C. Singh and P. A. Kollman, *J. Comput. Chem.*, 1984, **5**, 129–145; (*f*) B. H. Besler, K. M. Merz Jr and P. A. Kollman, *J. Comput. Chem.*, 1990, **11**, 431–439; (*g*) C. M. Breneman and K. B. Wiberg, *J. Comput. Chem.*, 1990, **11**, 361–373; (*h*) J. Cioslowski, *J. Am. Chem. Soc.*, 1989, **111**, 8333–8336.

17 (*a*) L. Xue and Z. Lin, *Chem. Soc. Rev.*, 2010, **39**, 1692–1705; (*b*) M. García-Melchor, A. A. C. Braga, A. Lledós, G. Ujaque and F. Maseras, *Acc. Chem. Res.*, 2013, **46**, 2626–2634; (*c*) J. Lu, S. Donnecke, I. Paci and D. C. Leitch, *Chem. Sci.*, 2022, **13**, 3477–3488.

18 (*a*) K. Kubota and H. Ito, *Trends Chem.*, 2020, **2**, 1066–1081; (*b*) K. Kubota, *Bull. Chem. Soc. Jpn.*, 2023, **96**, 913–930; (*c*) A. Porcheddu, E. Colacino, L. De Luca and F. Delogu, *ACS Catal.*, 2020, **10**, 8344–8394; (*d*) S. L. James, C. J. Adams, C. Bolm, D. Braga, P. Collier, T. Friščić, F. Grepioni, K. D. M. Harris, G. Hyett, W. Jones, A. Krebs, J. Mack, L. Maini, A. G. Orpen, I. P. Parkin, W. C. Shearouse,

Open Access Article. Published on 28 juli 2025. Downloaded on 29.9.2025 23:58:57.
This article is licensed under a Creative Commons Attribution-NonCommercial 3.0 Unported Licence.

J. W. Steed and D. C. Waddell, *Chem. Soc. Rev.*, 2012, **41**, 413–447; (*e*) G.-W. Wang, *Chem. Soc. Rev.*, 2013, **42**, 7668–7700; (*f*) X. Yang, C. Wu, W. Su and J. Yu, *Eur. J. Org. Chem.*, 2022, **2022**, e202101440; (*g*) S. Hwang, S. Grätz and L. Borchardt, *Chem. Commun.*, 2022, **58**, 1661–1667; (*h*) P. Ying, J. Yu and W. Su, *Adv. Synth. Catal.*, 2021, **363**, 1246–1271; (*i*) K. J. Ardila-Fierro and J. G. Hernández, *ChemSusChem*, 2021, **14**, 2145–2162; (*j*) V. Martinez, T. Stolar, B. Karadeniz, I. Brekalo and K. Užarević, *Nat. Rev. Chem.*, 2023, **7**, 51–65; (*k*) N. Fantozzi, J.-N. Volle, A. Porcheddu, D. Virieux, F. García and E. Colacino, *Chem. Soc. Rev.*, 2023, **52**, 6680–6714; (*l*) I. R. Speight, K. J. Ardila-Fierro, J. G. Hernández, F. Emmerling, A. A. L. Michalchuk, F. García, E. Colacino and J. Mack, *Nat. Rev. Methods Primers*, 2025, **5**, 29; (*m*) C. Bolm and J. G. Hernández, *Angew. Chem., Int. Ed.*, 2019, **58**, 3285–3299; (*n*) X. Xin, J. Geng, D. Zhang, H. T. Ang, H. Wang, Y. Cheng, Y. Liu, R. W. Toh, J. Wu and H. Wang, *Nat. Synth.*, 2025, **4**, 177–187; (*o*) K. Kubota, Y. Pang, A. Miura and H. Ito, *Science*, 2019, **366**, 1500–1504.

19 J. D. Hicks, A. M. Hyde, A. M. Cuezva and S. L. Buchwald, *J. Am. Chem. Soc.*, 2009, **131**, 16720–16734.

20 T. Seo, T. Ishiyama, K. Kubota and H. Ito, *Chem. Sci.*, 2019, **10**, 8202–8210.

21 J. B. Johnson and T. Rovis, *Angew. Chem., Int. Ed.*, 2008, **47**, 840–871.

22 (*a*) K. Kubota and H. Ito, *Trends Chem.*, 2020, **2**, 1066–1081; (*b*) K. Kubota, *Bull. Chem. Soc. Jpn.*, 2023, **96**, 913–930; (*c*) A. Porcheddu, E. Colacino, L. De Luca and F. Delogu, *ACS Catal.*, 2020, **10**, 8344–8394; (*d*) S. L. James, C. J. Adams, C. Bolm, D. Braga, P. Collier, T. Friščić, F. Grepioni, K. D. M. Harris, G. Hyett, W. Jones, A. Krebs, J. Mack, L. Maini, A. G. Orpen, I. P. Parkin, W. C. Shearouse, J. W. Steed and D. C. Waddell, *Chem. Soc. Rev.*, 2012, **41**, 413–447; (*e*) G.-W. Wang, *Chem. Soc. Rev.*, 2013, **42**, 7668–7700; (*f*) X. Yang, C. Wu, W. Su and J. Yu, *Eur. J. Org. Chem.*, 2022, **2022**, e202101440; (*g*) S. Hwang, S. Grätz and L. Borchardt, *Chem. Commun.*, 2022, **58**, 1661–1667.

23 N. W. J. Scott, M. J. Ford, N. Jeddi, A. Eyles, L. Simon, A. C. Whitwood, T. Tanner, C. E. Willans and I. J. S. Fairlamb, *J. Am. Chem. Soc.*, 2021, **143**, 9682–9693.

24 M. Rickhaus, L. M. Bannwart, M. Neuburger, H. Gsellinger, K. Zimmermann, D. Häussinger and M. Mayor, *Angew. Chem., Int. Ed.*, 2014, **53**, 14587–14591.

25 M. Rickhaus, L. M. Bannwart, O. Unke, H. Gsellinger, D. Häussinger and M. Mayor, *Eur. J. Org Chem.*, 2015, **2015**, 786–801.

26 M. Rickhaus, O. T. Unke, R. Mannancherry, L. M. Bannwart, M. Neuburger, D. Häussinger and M. Mayor, *Chem.–Eur. J.*, 2015, **21**, 18156–18167.

27 T. Seo, N. Toyoshima, K. Kubota and H. Ito, *J. Am. Chem. Soc.*, 2021, **143**, 6165–6175.

28 M. Tobisu, A. Yasutome, H. Kinuta, K. Nakamura and N. Chatani, *Org. Lett.*, 2014, **16**, 5572–5575.

29 A preliminary attempt showed that our catalytic system leads to moderate site-selectivity (C2/C4 = 63 : 27) in the Suzuki–Miyaura cross-coupling of 2,4-dibromotoluene with phenyl boronic acid without further optimization.

 © 2025 The Author(s). Published by the Royal Society of Chemistry